Chem Biol Drug Des 2014

Research Article

Design, Synthesis, and Biological Evaluation of Novel Quinazoline Derivatives as Anti-inflammatory Agents against Lipopolysaccharide-induced Acute Lung Injury in Rats

Jie Hu[1,†], Yali Zhang[1,†], Lili Dong[2], Zhe Wang[1], Lingfeng Chen[1], Dandan Liang[1], Dengjian Shi[1], Xiaoou Shan[2] and Guang Liang[1,*]

[1]Chemical Biology Research Center, School of Pharmaceutical Sciences, Wenzhou Medical University, University Town, Wenzhou, Zhejiang 325035, China
[2]Department of Pediatric, Second Affiliated Hospital of Wenzhou Medical University, 109 Xueyuan Road, Wenzhou, Zhejiang 325027, China
**Corresponding author: Guang Liang, wzmcliangguang@163.com*
[†]These authors contribute equally to this work.

Quinazoline has been reported to exhibit multiple bioactivities. The aim of this study was to discover new quinazoline derivatives with preventive effect on lipopolysaccharide-induced acute lung injury via anti-inflammatory actions. Thirty-three 4-amino quinazolin derivatives were synthesized and screened for anti-inflammatory activities in lipopolysaccharide-induced macrophages. The most potent four compounds, 6h, 6m, 6p, and 6q, were shown dose-dependent inhibition against lipopolysaccharide-induced TNF-α and IL-6 release. Then, the preliminary structure–activity relationship and quantitative structure–activity relationship analyses were conducted. To further determine the effects of quinazolines on acute lung injury treatment, lipopolysaccharide-induced acute lung injury model was employed. Male Sprague Dawley rats were pretreated with 6m or 6q before instillation of lipopolysaccharide. The results showed that 6m and 6q, especially 6q, obviously alleviated lung histopathological changes, inflammatory cells infiltration, and cytokines mRNA expression initiated by lipopolysaccharide. Taken together, this work suggests that 6m and 6q suppressed the lipopolysaccharide-induced acute lung injury through inhibition of the inflammatory response in vivo and in vitro, indicating that quinazolines might serve as potential agents for the treatment of acute lung injury and deserve the continuing drug development and research.

Key words: acute lung injury, anti-inflammation, IL-6, quinazoline derivatives, TNF-α

Received 10 August 2014, revised 12 October 2014 and accepted for publication 12 October 2014

Acute lung injury (ALI) is a clinical syndrome characterized by acute inflammatory process that includes neutrophil accumulation, interstitial edema, and lung parenchymal injury (1). It occurs mostly in young and is responsible for thousands of adult and pediatric deaths annually worldwide (2). Despite increasing insights into ALI, it still presents the high mortality rate of 30–40% and there are still few effective measures and special drugs to treat it (1,3,4). Therefore, the development of novel therapies for ALI is urgently needed. Recently, evidence from various clinical studies indicates that a complex network of inflammatory cytokines and chemokines plays a major role in lung injury process (5). Thus, treatments aimed at alleviating non-specific inflammatory reactions may have potential therapeutic.

Numerous inflammatory mediators are involved in ALI. Among them, IL-6 and TNF-α are considered the most important ones in innate immune response (6). IL-6 is a well-recognized inflammatory mediator upregulated in patients with ALI (7). Upon exposure to lipopolysaccharide (LPS), the lungs become a major source of systemic IL-6 as they become more permeable, allowing the facile translocation of IL-6 into the systemic circulation (8). TNF-α is the most extensively studied cytokine member of TNF superfamily. *In vivo*, excess generation of TNF-α facilitates pro-inflammatory reactions (9). Increasing evidence has emerged that excessive TNF-α production contributes to the deterioration of inflammation in ALI, and elevated levels of TNF-α has been found in bronchoalveolar lavage fluid (BALF) from patients with ALI (10). Therefore, the inhibition of the excessive production of pro-inflammatory cytokines, especially TNF-α and IL-6, stands as a central therapeutic strategy for ALI.

Quinazoline represents an interesting group of heterocycles, which exhibit various biological activities including containment of inflammatory disorders such as osteoarthritis (11), neurodegenerative impairments (12), and inflammatory bowel syndrome (13), invoking the interest in

 doi: 10.1111/cbdd.12454

synthesis and evaluation of their analogs. Additionally, different known anti-inflammatory drugs such as proquazone, fluoroquazone, and tryptanthrin are bearing quinazolinone nucleus (Figure 1). Also, it has been reported that some quinazoline derivatives possess potent anti-inflammatory activity, especially inhibit NF-κB transcriptional activation (14–16). Yet the relationship between anti-inflammatory activity and structure of quinazoline remains uncertain. Moreover, although numerous studies have addressed the cytokine-inhibitory potential of quinazoline derivatives, its ability to attenuate LPS-induced ALI remains poorly understood. In this study, we synthesized a novel series of quinazolinone derivatives, discussed the structure–activity relationship, and evaluated the anti-inflammatory activity. Active compounds were selected for the assessment of their vivo anti-inflammatory effects on LPS-induced ALI model.

Experimental Section

Chemical Synthesis

Materials and Methods

In general, reagents, solvents, and other chemicals were used as purchased without further purification. 5-Nitroanthranilonitrile (**1**), dimethylformamide dimethyl acetal (**2**), and various substituted aniline (**4a-4n**) were purchased from Alfa Aesar or Sigma–Aldrich. Other chemicals were obtained from local suppliers and were used without further purification. All reactions were monitored by thin-layer chromatography (250 silica gel 60 F_{254} glass plates). ^{1}H-NMR and ^{13}C-NMR spectra were recorded on Bruker 600 MHz instruments, and the chemical shifts were presented in terms of parts per million with TMS as the internal reference. Electron-spray ionization mass spectra in positive mode (ESI-MS) data were obtained with a Bruker Esquire 3000^{+} spectrometer. Chromatographic purification was carried out on Silica Gel 60 (E. Merck, 70–230 mesh).

***N*-(2-cyano-4-nitrophenyl)-*N,N*-dimethylformamide (3).** 5-Nitroanthranilonitrile **1** (4.89 g, 30 mM) and dimethylformamide dimethyl acetal (5.36 g, 45 mM) in toluene (50 mL) and the mixture was refluxed for 2 h. The resulting mixture was cooled to room temperature and refrigerated overnight. The yellow precipitate that formed was filtered, washed with ethyl ether, and dried to yield 6.0 g product (89.7%).

N-(3-fluorophenyl)-6-nitroquinazolin-4-amine (5a). A mixture of **3** (218.21 mg, 1 mM) and 3-fluoroaniline (**4a**, 1 mM) was heated and stirred at reflux in acetic acid (10 mL) for 1 h. The yellow precipitate that formed was filtered hot, washed with hot acetic acid, diethyl ether, and dried to give the desired nitroquinazoline **5a** as light yellow solid (180 mg, rate 63.2%). m.p: 230.7–232.6 °C (227–229 °C, lit.(17)). ESI-MS m/z: 284.8 $(M)^{+}$, 306.8 $(M+Na)^{+}$.

N-(3-chlorophenyl)-6-nitroquinazolin-4-amine (5b). By the procedure described above for **5a** using **3** (218.21 mg, 1 mM) and 3-chloroaniline (**4b**, 127.57 mg, 1 mM) to give 233 mg (77.7%) of yellow powder. m.p: 276.0–279.0 °C (278–281 °C, lit.(17,18)). ESI-MS m/z: 300.8 $(M)^{+}$.

N-(3-bromophenyl)-6-nitroquinazolin-4-amine (5c). By the procedure described above for **5a** using **3** (1091 mg, 5 mM) and 3-bromoaniline (**4c**, 851 mg, 5 mM) to give 1470 mg (85.0%) of yellow powder. m.p: 268.4–271.3 °C (267–270 °C, lit.(18,19)). ESI-MS m/z: 346.8 $(M)^{+}$.

6-nitro-N-(3-(trifluoromethyl)phenyl)quinazolin-4-amine (5d). By the procedure described above for **5a** using **3** (218.21 mg, 1 mM) and 3-trifluoromethylaniline (**4d**, 161.12 mg, 1 mM) to give 193.1 mg (57.8%) of yellow powder. m.p: 203.8–205.2 °C (203–205 °C, lit.(17)). ESI-MS m/z: 334.9 $(M)^{+}$.

6-nitro-N-(3,4,5-trifluorophenyl)quinazolin-4-amine (5e). By the procedure described above for **5a** using **3** (218.21 mg, 1 mM) and 3,4,5-trifluoroaniline (**4e**, 147 mg, 1 mM) to give 150.7 mg (47.1%) of yellow powder. m.p: 277.4–278.5 °C. ^{1}H-NMR (600 MHz, DMSO-d6) δ(p.p.m.): 9.527(s, 1H, Ar-H), 8.766 (s,1H, -N=CH-N-), 8.541 (d, J = 9.0 Hz, 1H, Ar-H), 7.927 (d, J = 9.0 Hz, 1H, Ar-H), 7.857–7.885(m, 2H, Ar-H).^{13}C-NMR(600 MHz, DMSO-d6) d(p.p.m.):106.47, 106.64, 114.44, 120.52, 126.73, 129.57, 135.33, 144.66, 148.94, 149.00, 150.58, 152.75, 157.06, 158.29. ESI-MS m/z: 320.8$(M)^{+}$, 342.8 $(M+Na)^{+}$.

N-(3-ethynylphenyl)-6-nitroquinazolin-4-amine (5f). By the procedure described above for **5a** using **3** (218.21 mg, 1 mM) and 3-aminophenylacetylene (**4f**,

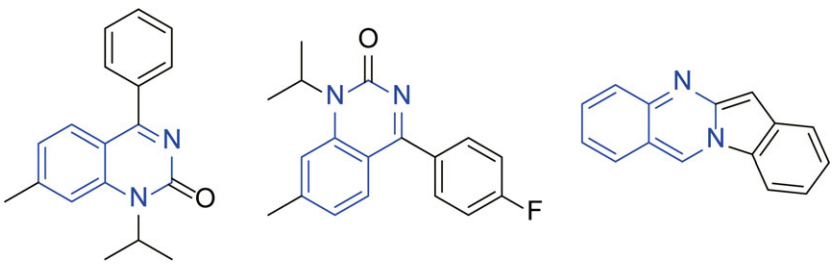

Proquazone Fluoroquazone Tryptanthrin

Figure 1: Several anti-inflammatory drugs bearing quinazolinone nucleus.

117 mg, 1 mM) to give 195 mg (67.2%) of yellow powder. m.p: 272.2–274.1 °C (271–272 °C, lit.(20)). ESI-MS m/z: 290.8 $(M)^+$.

6-nitro-N-(m-tolyl)quinazolin-4-amine (5g). By the procedure described above for **5a** using **3** (218.21 mg, 1 mM) and 3-methylaniline (**4g**, 107 mg, 1 mM) to give 208.6 mg (74.4%) of yellow powder. m.p: 247.6–249.3 °C (250–252 or 267–270 °C, lit.(18,21)). ESI-MS m/z: 280.8 $(M)^+$, 302.8 $(M+Na)^+$.

N-(4-morpholinophenyl)-6-nitroquinazolin-4-amine (5h). By the procedure described above for **5a** using **3** (218.21 mg, 1 mM) and 4-morpholinoaniline (**4h**, 90 mg, 0.5 mM) to give 152 mg (86.6%) of red powder. m.p: 281.0–282.7 °C (lit. (22)). ESI-MS m/z: 352.0 $(M)^+$.

N-(4-ethoxyphenyl)-6-nitroquinazolin-4-amine (5i). By the procedure described above for **5a** using **3** (218.21 mg, 1 mM) and 4-ethoxyaniline (**4i**, 137 mg, 1 mM) to give 211.7 mg (68%) of red powder. m.p: 203.0–205.8 °C (lit.(23)). ESI-MS m/z: 310.9 $(M)^+$, 332.9 $(M+Na)^+$.

N-(2,5-dimethoxyphenyl)-6-nitroquinazolin-4-amine (5j). By the procedure described above for **5a** using **3** (218.21 mg, 1 mM) and 2,5-dimethoxyaniline (**4j**, 153 mg, 1 mM) to give 305 mg (93.6%) of organic powder. m.p: 187.0–189.6 °C (lit.(24)). ESI-MS m/z: 326.9 $(M)^+$, 348.8 $(M+Na)^+$.

6-nitro-N-(3,4,5-trimethoxyphenyl)quinazolin-4-amine (5k). By the procedure described above for **5a** using **3** (218.21 mg, 1 mM) and 3,4,5-trimethoxyaniline (**4k**, 183 mg, 1 mM) to give 160 mg (45%) of red powder. m.p: 230.2–231.2 °C (258 °C, lit.(25)). ESI-MS m/z: 356.9 $(M)^+$, 378.9 $(M+Na)^+$.

N-(3,5-dimethoxyphenyl)-6-nitroquinazolin-4-amine (5l). By the procedure described above for **5a** using **3** (218.21 mg, 1 mM) and 3,5-dimethoxyaniline (**4l**, 153 mg, 1 mM) to give 301 mg (92.2%) of red powder. m.p: 223.2–224.8 °C (220 °C, lit.(25)). ESI-MS m/z: 326.9 $(M)^+$, 348.8 $(M+Na)^+$.

6-nitro-N-(quinolin-6-yl)quinazolin-4-amine (5m). By the procedure described above for **5a** using **3** (436 mg, 2 mM) and 6-aminoquinoline (**4m**, 288 mg, 2 mM) to give 432 mg (68%) of yellow powder. m.p: >300 °C (333–335 °C, lit. (26)). ESI-MS m/z: 317.9 $(M)^+$.

N-(6-chloropyridin-2-yl)-6-nitroquinazolin-4-amine (5n). By the procedure described above for **5a** using **3** (436 mg, 2 mM) and 2-amino-6-chloropyridine (**4n**, 256 mg, 2 mM) to give 328 mg (51.7%) of yellow powder. m.p: 249.0–251.5 °C. ^{1}H-NMR (600 MHz, DMSO-d6) δ(p.p.m.): 11.382 (s, 1H, -NH), 9.884 (s, 1H, Ar-H), 8.873 (s, 1H, N=CH-N), 8.585 (d, J = 9.6 Hz,1H, Ar-H), 8.423 (d, J = 6.6 Hz, 1H, Ar-H), 8.000 (d, J = 8.4 Hz, 1H, pyridine-H), 7.939–7.966 (m, 1H, pyridine-H), 7.305 (d, J = 7.2 Hz, 1H, pyridine-H). ^{13}C-NMR (600 MHz, DMSO-d6) d (p.p.m.):115.31, 119.53, 121.58, 122.99, 124.58, 126.96, 129.63, 130.00, 141.25, 144.25, 147.91, 157.07, 165.78. ESI-MS m/z: 301.8 $(M+H)^+$.

N-(1-methyl-1H-indol-5-yl)-6-nitroquinazolin-4-amine (5o). By the procedure described above for **5a** using **3** (218.21 mg, 1 mM) and 1-methyl-1H-indol-5-amine (**4o**, 146 mg, 1 mM) to give 179 mg (56.1%) of red powder. m.p: 241.2–242.8 °C. ^{1}H-NMR (600 MHz, DMSO-d6) δ (p.p.m.): 10.463 (s, 1H, -NH), 9.669 (d, J = 2.4 Hz, 1H, Ar-H), 8.617 (s, 1H, Ar-H), 8.524 (d, J = 9.0 Hz, 1H, Ar-H), 7.955 (s, 1H, -N=C-N-), 7.885 (d, J = 9.0 Hz, 1H, Ar-H), 7.475 (d, J = 8.4 Hz, 1H, Ar-H), 7.452 (d, J = 9.0 Hz, 1H, Ar-H), 7.358 (d, J = 3.0 Hz,1H, indole-H), 6.459 (d, J = 3.0 Hz, 1H, indole-H), 3.745(s, 3H, $-CH_3$). ^{13}C-NMR (600 MHz, DMSO-d6) d (p.p.m.): 32.59, 100.45, 109.43, 114.39, 115.42, 118.27, 120.87, 126.37, 127.76, 129.26, 129.98, 130.39, 134.18, 144.29, 153.17, 158.07, 159.12. ESI-MS m/z: 319.8 $(M)^+$, 341.7 $(M+Na)^+$.

6-nitro-N-(1-propyl-1H-indol-5-yl)quinazolin-4-amine (5p). By the procedure described above for **5a** using **3** (436 mg, 2 mM) and 1-propyl-1H-indol-5-amine (**4p**, 348 mg, 2 mM) to give 316 mg (45.5%) of red powder. m.p:183.6–185.2 °C. ^{1}H-NMR (600 MHz, DMSO-d6) δ (p.p.m.): 10.459 (s, 1H, -NH), 9.667 (d, J = 2.4 Hz, 1H, Ar-H), 8.614 (s, 1H, Ar-H), 8.527 (d, J = 9.0 Hz, 1H, Ar-H), 7.937(s, 1H, -N=CH-N-), 7.887 (d, J = 9.0 Hz, 1H, Ar-H), 7.517 (d, J = 9.0 Hz, 1H, Ar-H), 7.426 (d, J = 8.4 Hz, 1H, Ar-H), 7.407 (d, J = 3.0 Hz, 1H, indole-H), 6.463 (d, J = 3.0 Hz, 1H, indole-H), 4.112–4.166(m, 2H, N-CH_2-), 1.783–1.819 (m, 2H, -CH_2-), 0.846–0.870 (m, 3H, -CH_3). ^{13}C-NMR (600 MHz, DMSO-d6) d (p.p.m.): 11.18, 23.20, 47.20, 100.52, 109.57, 114.38, 115.55, 118.24, 120.87, 126.38, 127.80, 129.27, 129.39, 129.49, 133.55, 144.30, 153.18, 158.08, 159.15. ESI-MS m/z: 348.0$(M+H)^+$.

N-(1-allyl-1H-indol-5-yl)-6-nitroquinazolin-4-amine (5q). By the procedure described above for **5a** using **3** (278 mg, 1.28 mM) and 1-allyl-1H-indol-5-amine (**4q**, 220 mg, 1.28 mM) to give 175 mg (39.6%) of red powder. m.p: 229.1–230.1 °C. ^{1}H-NMR (600 MHz, DMSO-d6) δ (p.p.m.): 10.463 (s, 1H, -NH), 9.665 (d, J = 2.4 Hz, 1H, Ar-H), 8.617 (s, 1H, Ar-H), 8.519–8.538 (d, J = 9.0 Hz, 1H, Ar-H), 7.955 (s, 1H, -N=C-N-), 7.467 (d, J = 8.4 Hz, 1H, Ar-H), 7.467 (d, J = 9.0 Hz, 1H, Ar-H), 7.429 (d, J = 8.4 Hz, 1H, Ar-H), 7.384 (d, J = 3.0 Hz,1H, indole-H), 6.502 (d, J = 3.0 Hz, 1H, indole-H), 6.001–6.064 (m, 1H, C-CH=C), 5.169 (d, J = 10.2 Hz, 1H, -C=CH_2), 5.048 (d, J = 14.8 Hz,1H, -C=CH_2), 4.849 (d, J = 5.4 Hz, 2H,

N-CH_2-). ^{13}C-NMR (600 MHz, DMSO-d6) d (p.p.m.): 48.17, 106.97, 109.80, 114.38, 115.57, 116.66, 118.38, 120.87, 126.39, 127.94, 129.29, 129.51, 130.08, 133.53, 134.46, 144.30, 153.17, 158.10, 159.15. ESI-MS m/z: 346.1$(M+H)^+$.

N^4-(3-fluorophenyl)quinazoline-4,6-diamine (6a). 6-Nitroquinazoline **5a** (142 mg, 0.5 mM, 1.0 equiv) and iron (140 mg, 2.5 mM, 5.0 equiv) were suspended in aqueous ethanol (13 mL, 70% v/v) containing acetic acid (0.45 mL, 7 mM, 14 equiv) and heated at reflux until disappearance of starting material. The reaction mixture was cooled to room temperature and alkalinized by addition of concentrated ammonia or NaOH until the pH is adjusted to 8–9. Insoluble material was removed by filtration through celite, and the filtrate was evaporated under reduced pressure. The water phase was extracted twice with ethyl acetate, and the organic extracts were washed with brine, dried over $MgSO_4$, and concentrated under reduced pressure without heating. Chromatography on silica gel eluting with a mixture of ethyl acetate/petroleum ether gave the expected product with 52.2% yield (66.3 mg). m.p: 128.2–129.5 °C (122–124 °C, lit.(17)). ESI-MS m/z: 254.7$(M)^+$.

N^4-(3-chlorophenyl)quinazoline-4,6-diamine (6b). Celadon powder, 51.9% yield. m.p: 162.2–163.2 °C (235–237 °C or 186–189 °C, lit.(18,27)). ESI-MS m/z: 270.7$(M)^+$.

N^4-(3-bromophenyl)quinazoline-4,6-diamine (6c). Celadon powder, 77.9% yield. m.p: 199.1–200.4 °C (204–206 °C, lit.(18,19)). ESI-MS m/z: 314.8, 316.7$(M)^+$.

N^4-(3-(trifluoromethyl)phenyl)quinazoline-4,6-diamine (6d). Celadon powder, 37.5% yield. m.p: >250 °C (>250 °C, lit.(17,27,28)). ESI-MS m/z: 304.9$(M)^+$.

N^4-(3,4,5-trifluorophenyl)quinazoline-4,6-diamine (6e). Celadon powder, 30.1% yield. m.p:245.1–247.8 °C. ^{1}H-NMR (600 MHz, DMSO-d6) δ(p.p.m.): 9.575 (s, 1H, -NH), 8.418 (s,1H, -N=CH-N-), 7.939 (s, 2H, Ar-H), 7.570(d, J = 7.2 Hz, 1H, Ar-H), 7.284 (s, 2H, Ar-H), 5.683 (s, 2H, -NH_2). ^{13}C-NMR (600 MHz, DMSO-d6) d (p.p.m.): 100.44, 104.90, 105.06, 116.62, 124.08, 128.86, 136.56, 136.63, 142.75, 147.57, 149.20, 149.23, 150.60, 155.43. ESI-MS m/z: 290.9$(M)^+$.

N^4-(3-ethynylphenyl)quinazoline-4,6-diamine (6f). Celadon powder, 30.8% yield. m.p:250.0–251.2 °C (lit. (29)). ESI-MS m/z: 260.7$(M)^+$.

N^4-(m-tolyl)quinazoline-4,6-diamine (6g). Celadon powder, 62.2% yield. m.p:164.5–167.4 °C (245–248 °C or 173–175.5 °C, lit.(18,27)). ESI-MS m/z: 250.7$(M)^+$.

N^4-(4-morpholinophenyl)quinazoline-4,6-diamine (6h). Celadon powder, 18.2% yield. m.p: 230.2–232.4 °C (lit. (30)). ESI-MS m/z: 321.9$(M)^+$.

N^4-(4-ethoxyphenyl)quinazoline-4,6-diamine (6i). Celadon powder, 78.3% yield, m.p:160.1–161.2 °C. ^{1}H-NMR (600 MHz, DMSO-d6) δ (p.p.m.): 9.291 (s, 1H, -NH), 8.330 (s, 1H, N=CH-N), 7.669–7.776 (m, 2H, Ar-H), 7.486–7.517 (m, 1H, Ar-H), 7.351 (s, 1H, Ar-H), 7.209–7.228 (m, 1H, Ar-H), 6.911–6.948 (m, 2H, Ar-H), 5.537 (s, 2H, -NH_2), 4.000–4.043 (m, 2H, O-CH_2), 1.357–1.319 (m, 3H, -CH_3). ^{13}C-NMR (600 MHz, DMSO-d6) d (p.p.m.): 14.71, 63.13, 101.35, 114.12, 114.12, 116.25, 123.67, 124.13, 124.13, 127.04, 132.15, 147.51, 149.29, 154.93, 156.52, 162.67. ESI-MS m/z: 280.8$(M)^+$.

N^4-(quinolin-6-yl)quinazoline-4,6-diamine (6m). Celadon powder, 58.5% yield, m.p: 237.4–239.2 °C. ^{1}H-NMR (600 MHz, DMSO-d6) δ(p.p.m.): 9.658 (s, 1H, -NH), 8.778–8.784 (m, 1H, Ar-H), 8.581 (s, 1H, Ar-H), 8.423 (s, 1H, Ar-H), 8.3015 (d, 1H, J = 7.8 Hz, Ar-H), 8.188 (d, 1H, J = 9 Hz, Ar-H), 7.997 (d, 1H, J = 9 Hz, Ar-H), 7.571 (d, 1H, J = 9 Hz, Ar-H), 7.473–7.494 (m, 1H, Ar-H), 7.429 (s, 1H, Ar-H), 7.288–7.269 (m, 1H, Ar-H), 5.634 (s, 2H, -NH_2). ESI-MS m/z: 287.9 $(M)^+$.

N^4-(6-chloropyridin-2-yl)quinazoline-4,6-diamine (6n). Celadon powder, 34.2% yield, m.p: 206.3–209.8 °C. ^{1}H-NMR (600 MHz, DMSO-d6) δ(p.p.m.): 9.957 (s, 1H, -NH), 8.463 (s,1H, -N=C-N-), 8.391 (d, J = 8.6 Hz, 1H, Ar-H), 7.844–7.870 (m, 1H, Ar-H),7.584 (d, J = 9.0 Hz, 1H, Ar-H), 7.481 (s, 1H, Ar-H), 7.285 (d, J = 9.0 Hz, 1H, Ar-H), 7.157 (d, J = 7.8 Hz, 1H, Ar-H), 5.611 (s, 2H, -NH_2). ^{13}C-NMR (600 MHz,DMSO-d6) d (p.p.m.):101.16, 113.44, 116.95, 117.83, 124.21, 128.66, 140.98, 143.03, 147.62, 147.80, 149.12, 153.07, 155.00. ESI-MS m/z: 271.8$(M)^+$.

N^4-(1-methyl-1H-indol-5-yl)quinazoline-4,6-diamine (6o). Celadon powder, 41.7% yield. m.p: 217.4–219.6 °C. ^{1}H-NMR (600 MHz, DMSO-d6) δ(p.p.m.): 9.253 (s, 1H, -NH), 8.243 (s, 1H, N=CH-N), 7.976 (s, 1H, Ar-H), 7.490–7.505 (m, 1H, Ar-H), 7.443–7.461 (m, 1H, Ar-H), 7.394–7.408 (m, 2H, Ar-H), 7.300 (s, 1H, Ar-H), 7.226–7.207 (m, 1H, Ar-H), 6.411–6.415 (m, 1H, Ar-H), 5.488 (s, 2H, -NH_2), 3.790 (s, 3H, -CH_3). ^{13}C-NMR (600 MHz, DMSO-d6) d (p.p.m.): 32.60, 100.31, 101.39, 109.24, 114.48, 116.59, 118.19, 123.25, 127.86, 128.51, 130.05, 131.59, 133.64, 142.33, 147.02, 150.39, 156.72. ESI-MS m/z: 289.8 $(M)^+$.

N^4-(1-propyl-1H-indol-5-yl)quinazoline-4,6-diamine (6p). Celadon powder, 50.8% yield, mp 201.5–203.5 °C. ^{1}H-NMR (600 MHz, DMSO-d6) δ(p.p.m.): 9.232 (s, 1H, -NH), 8.223 (s, 1H, Ar-H), 7.943 (s, 1H, Ar-H), 7.493–7.350 (m, 4H, Ar-H), 7.214 (d, J = 2.4 Hz, 1H, indole-H), 7.200 (d, J = 2.4, 1H, indole-H), 6.412 (s, 1H, Ar-H), 5.477 (s, 2H, -NH_2), 4.119–4.142 (m, 2H, -CH_2-), 1.761–1. 809 (m, 2H, -CH_2-), 0.838–0.863 (m, 3H, -CH_3). ^{13}C-NMR (600 MHz, DMSO-d6) d (p.p.m.): 11.18, 23.20, 47.16, 100.28, 101.36, 109.29, 114.52, 116.54, 118.08, 123.16, 127.86, 128.45, 129.06, 131.46, 132.89, 142.31,

146.93, 150.30, 156.66. ESI-MS m/z: 318.1$(M+H)^+$, 340.0 $(M+Na)^+$.

N^4-(3-bromophenyl)-N^4-(3-methylbut-2-en-1-yl)quinazoline-4,6-diamine (6q). Celadon powder, 25.5% yield, mp 136.3–138.2 °C. ^{1}H-NMR (600 MHz, DMSO-d6) δ(p.p.m.): 9.239 (s, 1H, -NH), 8.227 (s, 1H, Ar-H), 7.965 (s, 1H, Ar-H), 7.486 (d, J = 9.1 Hz, Ar-H), 7.327–7. 425 (m, 4H, Ar-H), 7.199–7.217 (m, 1H, Ar-H), 6.450 (s, 1H, Ar-H), 5.999–6.044 (m, 1H, CH_2=CH-CH_2-), 5.480 (s, 2H, -NH_2), 5.168–5.21 (m, 2H, CH_2=CH-CH_2-), 4.821 (s, J = 5.4 Hz, 2H, CH_2=CH-CH_2-). ^{13}C-NMR (600 MHz, DMSO-d6) d (p.p.m.): 48.13, 100.75, 101.35, 109.53, 114.50, 116.55, 116.55, 118.18, 123.18, 127.95, 128.44, 129.09, 131.67, 132.87, 134.55, 142.29, 146.95, 150.27, 156.64. ESI-MS m/z: 316.0 $(M+H)^+$, 338.1 $(M+Na)^+$.

N-(1-allyl-1H-indol-5-yl)-6-nitroquinazolin-4-amine (7a). To a stirred solution of N-(3-bromophenyl)-6-nitroquinazolin-4-amine (**5c**, 347 mg, 1 mM) and allyl bromide (158 mg, 1.2 mM) in acetonitrile (10 mL) was added potassium carbonate (207 mg) and the mixture was refluxed at 80 °C. Stirring was continued for 8 h, and then, the solvent was evaporated and the crude was dissolved in EtOAc, followed by washed with saturated NH_4Cl, dried ($MgSO_4$), and evaporated. The residue was chromatographed on silica gel to give 300 mg (59%) of **7a** as a orange solid, m.p: 172.1–173.8 °C. ^{1}H-NMR (600 MHz, DMSO-d6) δ(p.p.m.): 8.928 (d, J = 3.0 Hz, 1H, Ar-H), 8.430 (d, 1H, J = 9.0 Hz, Ar-H), 8.123(s, 1H, N=CH-N), 7.588 (d, J = 9.6 Hz, 1H, Ar-H), 7.233–7.279 (m, 2H, Ar-H), 7.179 (d, J = 7.8 Hz, 1H, Ar-H), 7.036 (d, J = 7.8 Hz, 1H, Ar-H), 5.986–6.041 (m, 1H, C=CH-C), 5.243–5.284 (m, 2H, CH_2=C-), 4.773 (d, J = 4.8 Hz, 2H, -CH_2-). ^{13}C-NMR (600 MHz, DMSO-d6) d (p.p.m.): 50.98, 117.27, 118.13, 120.01, 121.14, 121.82, 121.86, 124.91, 125.12, 126.80, 130.20, 132.16, 142.32, 144.39, 151.48, 151.51, 152.14. ESI-MS m/z: 384.9$(M)^+$.

N-(1-allyl-1H-indol-5-yl)-6-nitroquinazolin-4-amine (7b). Using the procedure described for the preparation of **7a**, 284 mg (68.8%) of a orange solid was obtained from **5c** (347 mg, 1 mM) and 1-chloro-3-methylbut-2-ene (208 mg, 2 mM), m.p: 117.2–118.3 °C. ^{1}H-NMR (600 MHz, DMSO-d6) δ(p.p.m.): 8.920 (d, J = 2.4 Hz, 1H, Ar-H), 8.465 (d, 1H, J = 9.0 Hz, Ar-H), 8.141(s, 1H, N=CH-N), 7.513 (d, J = 9.6 Hz, 1H, Ar-H), 7.227–7.267 (m, 2H, Ar-H), 7.016–7.033 (m, 1H, Ar-H), 7.163–7.181 (m, 1H, Ar-H), 5.263–5.284 (m, 1H, -C=CH-C-), 4.715 (d, J = 6.6 Hz, 2H, -CH_2-), 1.823 (s, 3H, -CH_3), 1.718 (s, 3H, -CH_3). ^{13}C-NMR (600 MHz, DMSO-d6) d (p.p.m.): 18.09, 25.33, 47.57, 116.96, 118.22, 120.08, 121.13, 121.81, 121.87, 124.91, 125.06, 126.93, 130.19, 137.82, 142.25, 144.37, 151.59, 151.60, 151.83. ESI-MS m/z: 412.9 $(M)^+$.

Animals

ICR mice and Sprague Dawley (SD) rats aged 6 weeks were purchased from the Animal Center of Wenzhou Medical University (Wenzhou, China). Animals were housed at a constant room temperature with a 12:12 hour light–dark cycle and fed with a standard rodent diet and water. The animals were acclimatized to the laboratory for at least 7 days before used in experiments. Protocols involving the use of animals were approved by the Wenzhou Medical University Animal Policy and Welfare Committee (Approval documents: 2013/APWC/0361).

Cells and regents

Mouse peritoneal macrophages (MPMs) were isolated as descript in our previous study (31). Briefly, ICR mice were stimulated by an i.p. injection of 6% thioglycollate solution (0.3 g beef extract, 1 g tryptone, 0.5 g NaCl dissolved in 100 mL ddH_2O, and filtrated through 0.22-μm filter membrane, 1.5 mL per mouse) and kept in a pathogen-free condition for 3 days before MPM isolation. Total MPMs were harvested by washing the peritoneal cavity with RPMI-1640 medium (8 mL per mouse), centrifuged, and suspended in RPMI-1640 medium (Gibco/BRL life Technologies, Eggenstein, Germany) with 10% FBS (Hyclone, Logan, UT, USA), 100 U/mL penicillin, and 100 mg/mL streptomycin. Non-adherent cells were removed by washing with medium 3 h after seeding. Before treatment, MPMs were cultured in 35-mm plates and incubated overnight at 37 °C in a 5% CO_2-humidified air.

Human lung epithelial BEAS-2B cells were obtained from the American Type Culture Collection (Manassas, VA, USA). Cells were incubated in Dulbecco's modified Eagle's medium (Gibco®; Life Technologies, Carlsbad, CA, USA) supplemented with 10% fetal bovine serum (Gibco®; Life Technologies), 100 U/mL of penicillin, and 100 mg/mL of streptomycin at 37 °C with 5% CO_2. Lipopolysaccharide was purchased from Sigma (Louis, MO, USA). Mouse TNF-α and IL-6 enzyme-linked immunosorbent assay (ELISA) kits were purchased from eBioscience, Inc. (San Diego, CA, USA). All other chemicals were of reagent grade.

Enzyme-linked immunosorbent assay

Mouse peritoneal macrophages (5×10^5 per plate) in 35-mm plates were pretreated with 10 μM quinazoline derivatives for 30 min and stimulated with LPS (0.5 μg/mL) for 24 h. After treatment, the culture media and cells were collected separately. The levels of TNF-α and IL-6 in the media were determined by ELISA according to the manufacturers' instructions.

Quantitative structure–activity relationship analysis

The methods and software used for the quantitative structure–activity relationship (SAR) model establishment and analysis (including descriptor calculation and selection,

multiple linear regression analysis, and related software) were described in our previous publication (32).

Lipopolysaccharide-induced acute lung injury in rats

The 24 healthy male SD rats were randomly divided into four groups: control group, LPS group, **6m** plus LPS group, and **6q** plus LPS group. Each group contained six rats. **6m** and **6q** (20 mg/kg) were given orally for 7 days prior to administration of LPS. Rats from the control and LPS groups received an equal volume of 0.5% CMCNa. After being anesthetized by diethyl ether, mice were intratracheal instillation 50 μL LPS (20 μg/mL) to induce lung injury. Control rats were given 50 μL physiological saline. Twenty-four hours after LPS administration, animals were euthanized to collect BALF and lung tissue samples. Collection of BALF was performed three times through a tracheal cannula with autoclaved physiological saline, instilled up to a total volume of 3 mL.

Histopathological evaluation

Pulmonary tissues were harvested 24 h after the injection of LPS. Then, the samples were fixed with 4% paraformaldehyde for 24 h, embedded in paraffin, and sectioned (5 μm). The tissue-sectioned samples were stained with H&E and immunohistochemical. Pathological changes and inflammatory cell infiltration were observed under the light microscopy.

Bronchoalveolar lavage fluid collection, cell count, and protein concentration

Rats were anesthetized 24 h after being treated with LPS. Bronchoalveolar lavage fluid was performed three times by lavaged with of 1 mL of physiological saline. The lavage fluid was centrifuged, and the supernatants were used for analysis. Cell pellets were resuspended in 0.05 mL of physiological saline and used for total cell counts on a hemocytometer. Total protein concentration of BALF was measured using a bicinchoninic acid (BCA) assay kit (Pierce; Rockford, IL, USA) according to the manufacturer's instructions, with bovine serum albumin (BSA) as the standard.

Lung wet-to-dry weight (W/D) ratio

After rats were killed, the inferior lobe of right lungs was excised, blotted dry, weighed to obtain the 'wet' weight and then placed in an oven at 60 °C for 48 h to obtain the 'dry' weight. To quantify edema, the ratio of wet lung to dry lung was calculated.

Statistical analysis

Data are presented as mean ± SEM. Statistics were analyzed using Student's *t*-test mode in GRAPHPAD PRISM 5.0 (GraphPad, San Diego, CA, USA). p-Value <0.05 ($p < 0.05$) were considered as significance. All experiments were repeated more than three times.

Result and Discussion

Chemistry

A general synthetic approach was adopted for the rapid generation of C4 aniline quinazoline with nitro group or amino group at the 6-position of the quinazoline ring following the literature method (33). The synthetic route is depicted in Schemes 1 and 2. Briefly, 2-cyano-4-nitro-aniline **(1)** was reacted with N, N-dimethylformamide dimethyl acetal **(2)** to afford formamidine **3**. Cyclization of the intermediate **3** followed by corresponding amines in acetic acid and gave compounds **5a-5n** or **5o-5q.** Reduction of **5a-5j**, **5m**, **5n**, or **5o-5q** under the same condition composed of Fe/EtOH/AcOH provided **6a-6j**, **6m**, **6n**, and **6o-6q**, respectively. To investigate the effect of alkylation substituent on the R_2, compounds **7a** and **7b** were designed and prepared. The alkylation of N-(3-bromophenyl)-6-nitroquinazolin-4-amine **(5c)** with allyl bromide or 1-chloro-3-methylbut-2-ene in the presence of potassium carbonate gave compounds **7a** or **7b**, respectively. In addition, amines **4a-4n** were commercially available, while N-substituted aminoindoles **4o-4q** were prepared as procedure described in lit (33). The structures of all compounds were shown in Scheme 1 or 2. The new compounds were characterized by ^{1}H-NMR, ^{13}C-NMR, and electron-spray ionization mass spectrometry [ESI-MS].

Anti-inflammatory evaluation of quinazoline derivatives

To evaluate the anti-inflammatory effect of 33 synthetic quinazoline derivatives, we firstly monitored TNF-α and IL-6 secretion induced by LPS in MPMs with or without the pretreatment of compounds. Briefly, the cells were pretreated with target compounds at 10 μM or DMSO control for 30 min and then activated with LPS (0.5 μg/mL) for 24 h. Culture medium was collected and the amount of TNF-α and IL-6 release were measured by ELISA. The preliminary screening results are shown in Figure 2. A majority of 33 tested compounds exhibited significantly anti-inflammatory activity against LPS-induced TNF-α and IL-6 expression *in vitro*. Among these compounds, **5o**, **5q**, **6b**, **6m**, and **6o-6q** exhibited strong inhibitory abilities in IL-6 expression (inhibitory rate > 50%, Figure 2A). Meanwhile, four compounds, including **6h**, **6m**, **6p**, and **6q**, showed the inhibitory effect on TNF-α expression with an inhibition rate higher than 50% (Figure 2B). It is worth to note that compounds **6h**, **6m**, **6p**, and **6q** exhibited great inhibition against both TNF-α and IL-6 expression, so they were chosen for further study.

We draw a preliminary SAR conclusion from the result of anti-inflammatory screening. It is observed that

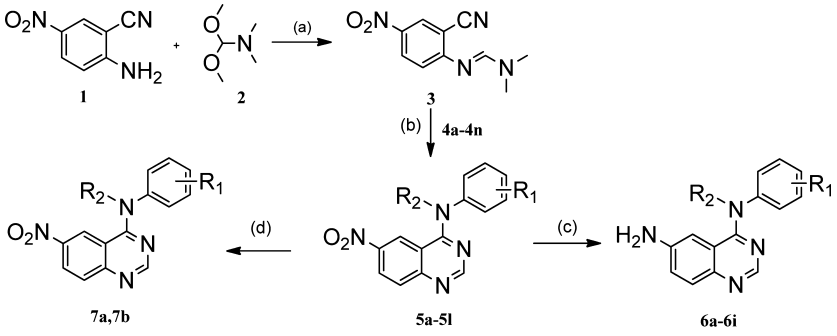

Comp.	R_1	R_2	Comp.	R_1	R_2
5a	3-F	H	**6a**	3-F	H
5b	3-Cl	H	**6b**	3-Cl	H
5c	3-Br	H	**6c**	3-Br	H
5d	3-CF_3	H	**6d**	3-CF_3	H
5e	3,4,5-F	H	**6e**	3,4,5-F	H
5f	3-C≡CH	H	**6f**	3-C≡CH	H
5g	3-CH_3	H	**6g**	3-CH_3	H
5h	4-morpholine	H	**6h**	4-morpholine	H
5i	4-ethyoxyl	H	**6i**	4-ethyoxyl	H
5j	2,5-OCH_3	H	**7a**	3-Br	allyl
5k	3,4,5-OCH_3	H	**7b**	3-Br	isopentene
5l	2,5-OCH_3	H			

Scheme 1: Synthetic and chemical structure of quinazoline derivatives **5a**-**5l**, **6a**-**6i,** and **7a**, **7b**. Reagents and conditions: (a) toluene, reflux, 2 h, 90%; (b) $ArNH_2$, AcOH, reflux, 3 h, 80–95%; (c) Fe, CH_3COOH, C_2H_5OH, 78 °C, reflux, 1 h, 50–85%; (d) K_2CO_3, CH_3CN, 80 °C, reflux, 8 h.

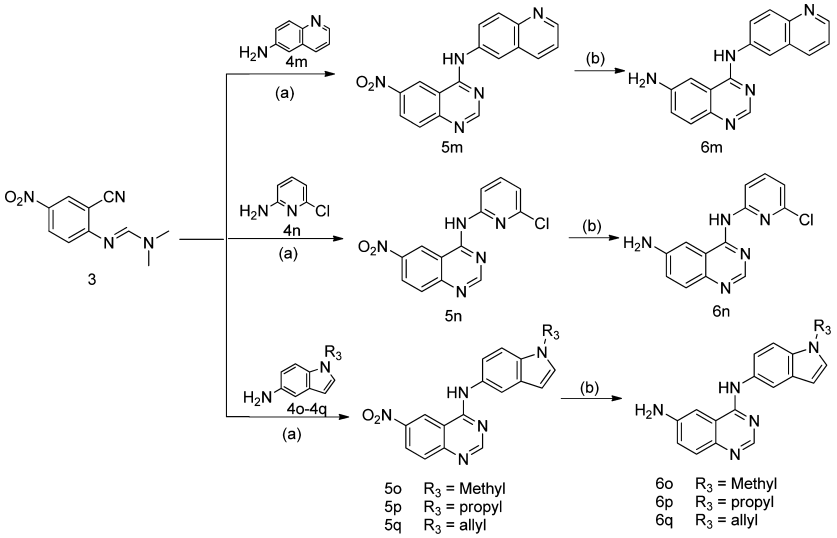

Scheme 2: Synthetic and chemical structure of quinazoline derivatives **5m**-**5q** and **6m**-**6q**. Reagents and conditions: (a) $ArNH_2$, AcOH, reflux, 3 h, 80–95%; (b) Fe, CH_3COOH, C_2H_5OH, 78 °C, reflux, 1 h, 50–85%.

compounds in series **6**, which has an amino group at the 6-position of the quinazoline ring, inhibited IL-6 and TNF-α release slightly stronger than those nitro derivatives (series **5**). The introduction of allyl or isopentene group at R_2 position (compounds **7a** and **7b**) could slightly increase the cytokine-inhibitory ability. On the

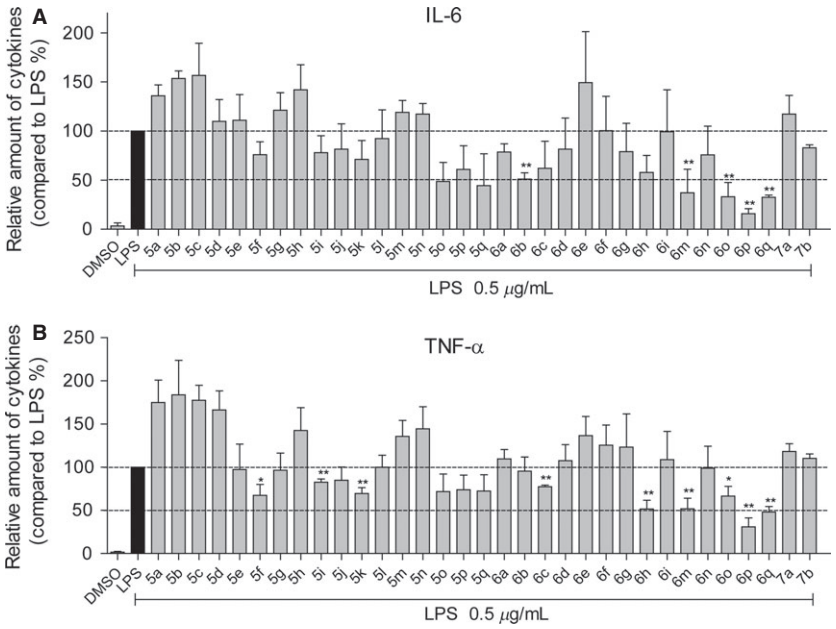

Figure 2: Quinazoline analogs inhibited lipopolysaccharide (LPS)-induced IL-6 (A) and TNF-α (B) secretion in mouse peritoneal macrophages. Macrophages were plated at a density of 5.0×10^5/plate at 37 °C, and 5% CO_2 overnight. Cells were pretreated with quinazoline analogs (10 μM) for 30 min, then treated with LPS (0.5 μg/mL) for 24 h. TNF-α and IL-6 levels in the culture media were measured by ELISA and were normalized by the total protein. The results were expressed as the percent of LPS control. Each bar represents mean ± SEM of 3 independent experiments. Statistical significance relative to LPS group was indicated, *p < 0.05, **p < 0.01.

other hand, the electronic properties of the substituents at R_1 site seem to have little influence on bioactivity. For example, compounds containing either electron-withdrawing group (**6b** and **6c**) or electron-donor moiety (**6h**) showed strong anti-inflammatory activity. It is noteworthy that the introduction of heterocycles or heterocyclic groups at 4-amino-phenyl position could enhance the anti-inflammatory activity, such as active compounds **5o-5q**, **6m**, and **6o-6q**.

Quantitative structure–activity relationship

To further explore and investigate the SAR of these compounds in the inhibition of TNF-α and IL-6 expression, a quantitative structure–activity relationship (QSAR) was calculated for 33 quinazoline derivatives. During a QSAR model study, the structure properties of compounds are often represented by their molecular descriptors. Statistically significant models with three variables were derived for anti-TNF-α and IL-6 activity, respectively. The scatter plot of predicted values versus experimental values is illustrated in Figure 3. The statistically significant models, Eq1 and Eq2, were obtained for anti-TNF-α and anti-IL-6 activities of compounds, with relatively high regression coefficients (R^2) of 0.71 and 0.74, respectively. The variables in the Eq1 model contained the geometrical molecular descriptor WHIM (Weighted Holistic Invariant Molecular Descriptor), 3D-MoRSE (3D Molecule Representation of Structures based on Electron diffraction Descriptor), and GETAWAY (GEometry, Topology, and Atom-Weights AssemblY Descriptor), while in the Eq2, the variables contained the geometrical molecular descriptors SAS (solvent-accessible surface) and GETAWAY and quantum chemistry descriptor EEVA (Electronic Eigenvalue Descriptor). A more detailed description of these molecular descriptors is provided in the experimental section. The QSAR results indicate that molecular electronegativity and molecular surface may play a pivotal role in the anti-inflammatory activity of these compounds. The result of QASR study can guide us to further design analogs with better bio-activity in the future study.

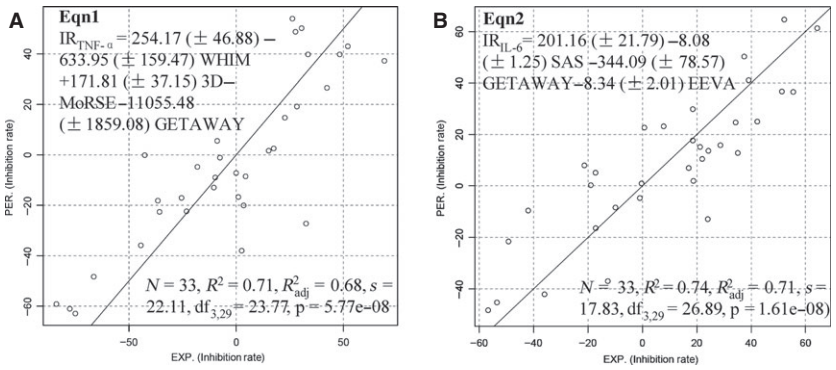

Figure 3: Plots of predicted activity against the corresponding experimental activity on TNF-α (A) and IL-6 (B) inhibition. N, the number of compounds taken into account in the regression; R^2, the multiple correlation coefficient; R_{adj}^2, adjusted multiple correlation coefficient; s, residual standard error; and the F value is related to the F-statistic analysis (Fisher's test). The numbers in parentheses mean the standard deviation of the coefficients.

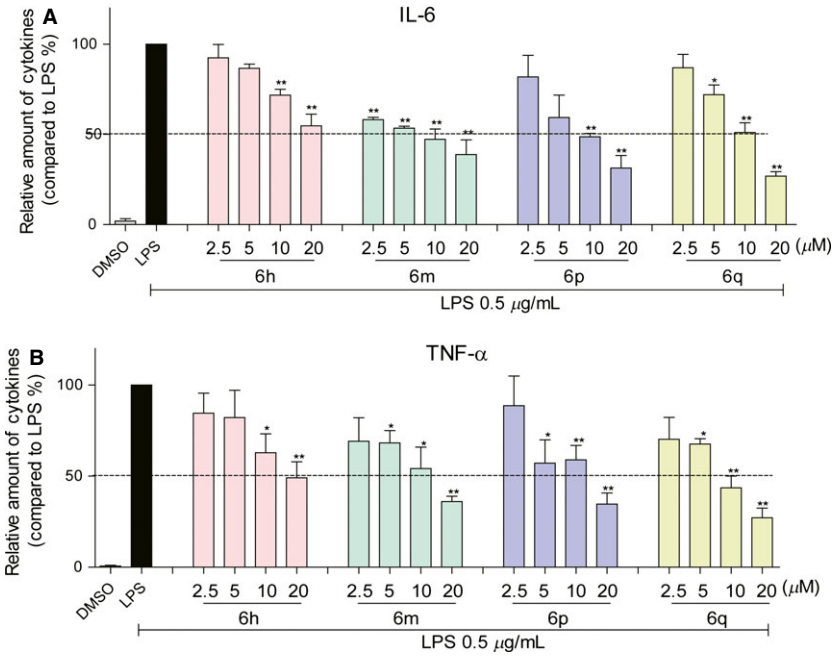

Figure 4: Four active compounds inhibited lipopolysaccharide (LPS)-induced IL-6 (A) and TNF-α (B) release in a dose-dependent manner. Mouse peritoneal macrophages were plated at a density of 5.0 × 10^5/plate at 37 °C, and 5% CO_2 overnight. Cells were pretreated with compounds at indicated concentrations (2.5, 5, 10, and 20 μM) for 30 min, then treated with LPS (0.5 μg/ml) for 24 h. IL-6 and TNF-α levels in the culture media were measured by ELISA and were normalized by the total protein. The results were expressed as the percent of LPS control. Each bar represents mean ± SEM of three independent experiments. Statistical significance relative to LPS group was indicated, *p < 0.05, **p < 0.01.

Active compounds inhibit TNF-α and IL-6 release in a dose-dependent manner

Among active compounds above, four compounds, **6h**, **6m**, **6p**, and **6q**, demonstrated the highest anti-inflammatory activities in MPMs. Thus, they were chosen for further evaluation of their dose-dependent inhibitory effects against LPS-induced TNF-α and IL-6 release. Macrophages were pretreated with **6h**, **6m**, **6p**, and **6q** in a series of

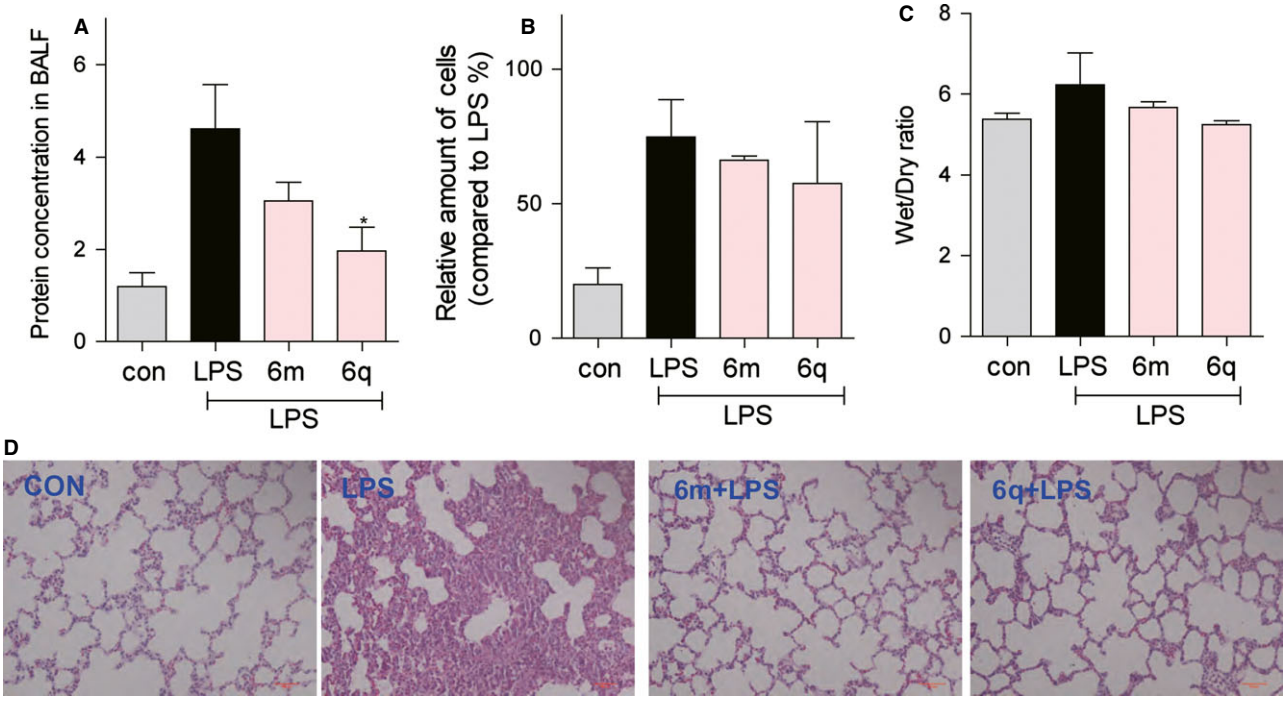

Figure 5: Effects of **6m** and **6q** on lipopolysaccharide (LPS)-mediated lung injury. Effects of **6m** and **6q** on the total protein concentration (A), the relative amount of cells in bronchoalveolar lavage fluid (B), and the lung W/D ratio (C) of LPS-induced ALI rats. (D) Effects of **6m** and **6q** on histopathological changes in lung tissues in ALI model induced by LPS. Rats were given an intragastric administration of **6m, 6q** (20 mg/kg/day), or CMCNa 7 days prior to an intranasal administration of LPS. Then, rats were anesthetized and lung tissue samples were collected at 24 h after LPS challenge for histological evaluation. These representative histological changes of the lung were obtained from rats of different groups (hematoxylin and eosin staining, original magnification 200 ×). *p < 0.05.

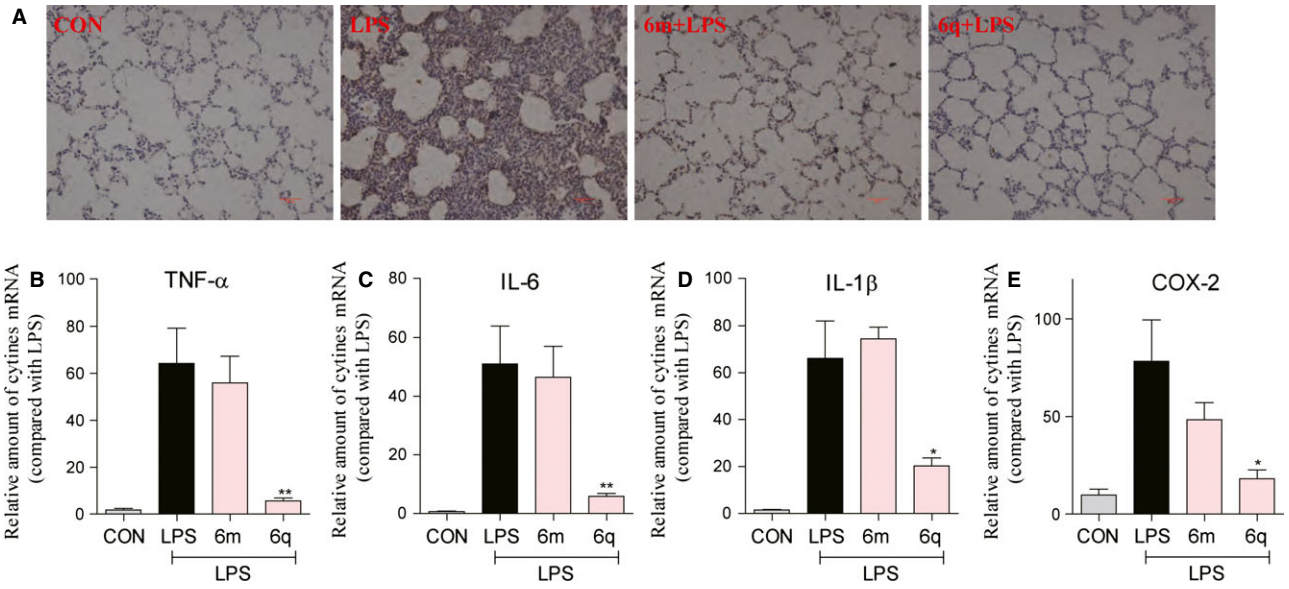

Figure 6: Effects of **6m** and **6q** on lipopolysaccharide (LPS)-mediated lung inflammation. (A) The changes of macrophage infiltration in lung tissues after LPS treatment and **6m** or **6q** pretreatment. The inhibition of **6m** and **6q** on the expression of inflammatory genes on lung tissue analyzed by mRNA assay. (B) TNF-α, (C) IL-6, (D) IL-1β, and (E) COX-2. Statistical significance relative to LPS group was indicated, *$p < 0.05$, **$p < 0.01$.

concentrations (2.5, 5, 10, and 20 μM) for 30 min and subsequently incubated with LPS (0.5 μg/mL) for 24 h. As shown in Figure 4, pretreatment with **6h**, **6m**, **6p**, and **6q** exhibited a dose-dependent inhibition on both TNF-α and IL-6 release induced by LPS. This further validates that these compounds have the potential to be used as anti-inflammatory agents.

Effects of 6 m and 6q on lipopolysaccharide-mediated lung pathophysiologic changes

Two derivatives **6m** and **6q** showing the highest anti-inflammatory activity were chosen for *in vivo* evaluation in rats with ALI induced by intratracheal instillation of LPS. The details of animal experiments were described in experimental section. Lipopolysaccharide has been widely used to induce the animal models of ALI, which resemble many characteristics of human ALI (34). Twenty-four hours after LPS administration, the rats were euthanized by chloral hydrate and the lung tissues and BALF were collected. Then, the lung wet/dry ratio, total protein concentration, and relative amount of cells in the BALF were evaluated. The results in Figure 5 indicated that LPS instillation significantly increased total protein concentration and relative amount of cells in BALF (Figure 5A,B). However, pretreatment with **6m** and **6q** obviously decreased the total protein concentration compared with LPS group. Meanwhile, **6m** and **6q** slightly inhibited relative amount of cells in the BALF (Figure 5B) and lung W/D ratio (Figure 5C).

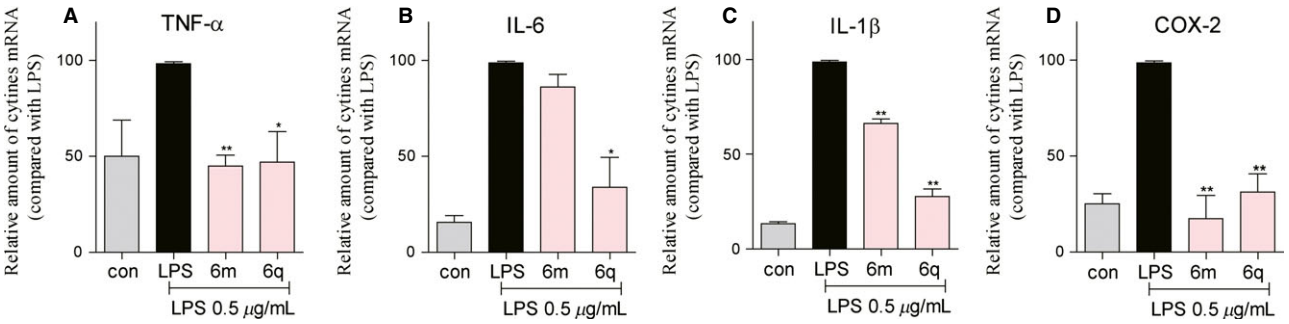

Figure 7: Effects of **6m** and **6q** on the expression of inflammatory genes in the human lung epithelial cells. The levels of TNF-α (A), IL-6 (B), IL-1β (C), and COX-2 (D) were measured by mRNA analysis. The results were expressed as the percent of lipopolysaccharide (LPS) control. Each bar represents mean ± SEM of 3 independent experiments. Statistical significance relative to LPS group was indicated, *$p < 0.05$, **$p < 0.01$.

To evaluate the histological changes in LPS-treated rats, lung tissues were subjected to H&E staining. Lung tissues from the control group showed a normal structure and no histopathological change under a light microscope (Figure 5D). Lipopolysaccharide instillation resulted in a significant inflammatory cells infiltration, thickening of the alveolar wall, and pulmonary congestion. However, LPS-induced pathological changes were significantly attenuated by either **6m** or **6q** treatment (Figure 5D). These results indicated that **6m** and **6q** had protective effect against LPS-induced ALI by reducing total protein concentration and attenuating histopathological changes.

6m and 6q reduce the expression of inflammatory genes in vivo *and* in vitro

To evaluate the effect of **6m** and **6q** on the LPS-induced inflammation in lung tissue, we examined the inflammatory cells infiltration and cytokines expression. Macrophages infiltration (Figure 6A) was studied by examining the CD68 immunostaining of lung tissue. Lipopolysaccharide treatment aggravated lung macrophages infiltration, which was significantly attenuated by pretreatment with **6m** or **6q**. Inflammatory cytokines mRNA levels in lung tissues were measured by real-time qPCR. The data showed that the expression of TNF-α, IL-6, IL-1β, and COX-2 was increased in the LPS alone group. However pretreatment with **6m** or **6q** inhibited the expression of these inflammatory genes (Figure 6B–E). Using the Beas-2B human lung epithelial cell line, we further confirmed the anti-inflammatory effects of **6m** and **6q**. Figure 7 showed that LPS markedly increased the inflammatory genes expression and preincubated **6m** (10 μM) markedly reduced the LPS-induced production of TNF-α, IL-1β, and COX-2 ($p < 0.01$), while **6q** (10 μM) obviously decreased the LPS-induced release of all four inflammatory genes ($p < 0.05$ or $p < 0.01$). There is no conclusion to account for the difference between **6m** and **6q** on LPS-induced mRNA expression, maybe the introduction of allyl group increase solubility behavior of **6q** leading to improved inhibition on the inflammatory genes expression. Taken together, **6m** and **6q**, especially **6q**, may protect against LPS-induced ALI by attenuating inflammatory response.

Acute lung injury is an acute inflammatory process in the airspaces and lung parenchyma injury involving the release of pro-inflammatory cytokines. Evidences from clinical studies indicated that a complex network of cytokines, including TNF-α, IL-1β, IL-6, and other pro-inflammatory mediators, initiates, amplifies, and perpetuates the inflammatory response in ALI (5). Increased levels of TNF-α, IL-1β, and IL-6 in the BALF have been noted in patients with ALI, and the persistent elevation of pro-inflammatory cytokines in humans with ALI has been associated with more severe outcomes (35). In the present study, LPS caused a significant increase in the mRNA levels of TNF-α, IL-6, IL-1β, and COX-2 both *in vivo* and *vitro,* while **6m** and **6q** pretreatment resulted in a significant decreased in the expression of these pro-inflammatory cytokines. These results suggested that the protective effect of **6m** and **6q** on LPS-induced ALI may be mainly attributed to their inhibition of inflammatory response.

Conclusion

In summary, 33 quinazoline derivatives were synthesized and their anti-inflammatory activities were evaluated in LPS-induced MPMs. A majority of these synthetic compounds exhibited significant anti-inflammatory activities, and the most potent ones, **6h**, **6m**, **6p**, and **6q**, inhibit both TNF-α and IL-6 release in a dose-dependent manner. Discussion and conclusions were made regarding structure–activity relationships. Further, *in vivo* experiment reveals that **6m** and **6q**, especially **6q**, could attenuate LPS-induced ALI in rats, via decreasing inflammatory cytokine production, protein concentration in the BALF, pathological changes, and macrophage infiltration. These present the possibility that quinazolines might serve as potential agents for the treatment of ALI. Although the anti-inflammatory mechanism and underlying targets are still unknown, the beneficial effects of these compounds on LPS-induced inflammation make quinazoline one of important leads in the continuing drug development and research.

Acknowledgments

Financial support was provided by the National Natural Science Funding of China (81302642 and 21272179), Zhejiang Provincial Natural Science Funding (LQ14H310003), High-level Innovative Talent Funding of Zhejiang Department of Health (G. L.), National '863' project (2011AA02A113).

References

1. Ware L.B., Matthay M.A. (2000) The acute respiratory distress syndrome. N Engl J Med;342:1334–1349.
2. Musumeci F., Radi M., Brullo C., Schenone S. (2012) Vascular endothelial growth factor (VEGF) receptors: drugs and new inhibitors. J Med Chem;55:10797–10822.
3. Hemmila M.R., Napolitano L.M. (2006) Severe respiratory failure: advanced treatment options. Crit Care Med;34:S278–S290.
4. Lee W.L., Downey G.P. (2001) Neutrophil activation and acute lung injury. Curr Opin Crit Care;7:1–7.
5. Goodman R.B., Pugin J., Lee J.S., Matthay M.A. (2003) Cytokine-mediated inflammation in acute lung injury. Cytokine Growth Factor Rev;14:523–535.
6. Meduri G.U., Kohler G., Headley S., Tolley E., Stentz F., Postlethwaite A. (1995) Inflammatory cytokines in the BAL of patients with ARDS. Persistent elevation over time predicts poor outcome. Chest;108:1303–1314.

7. Wang Y.L., Malik A.B., Sun Y., Hu S., Reynolds A.B., Minshall R.D., Hu G. (2011) Innate immune function of the adherens junction protein p120-catenin in endothelial response to endotoxin. J Immunol;186:3180–3187.
8. Schrader L.I., Kinzenbaw D.A., Johnson A.W., Faraci F.M., Didion S.P. (2007) IL-6 deficiency protects against angiotensin II induced endothelial dysfunction and hypertrophy. Arterioscler Thromb Vasc Biol;27: 2576–2581.
9. Ito H., Koide N., Hassan F., Islam S., Tumurkhuu G., Mori I., Yoshida T., Kakumu S., Moriwaki H., Yokochi T. (2006) Lethal endotoxic shock using alpha-galactosylceramide sensitization as a new experimental model of septic shock. Lab Invest;86:254–261.
10. Mukhopadhyay S., Hoidal J.R., Mukherjee T.K. (2006) Role of TNFalpha in pulmonary pathophysiology. Respir Res;7:125.
11. Rudolph J., Esler W.P., O'Connor S., Coish P.D., Wickens P.L., Brands M., Bierer D.E. *et al.* (2007) Quinazolinone derivatives as orally available ghrelin receptor antagonists for the treatment of diabetes and obesity. J Med Chem;50:5202–5216.
12. Iwashita A., Yamazaki S., Mihara K., Hattori K., Yamamoto H., Ishida J., Matsuoka N., Mutoh S. (2004) Neuroprotective effects of a novel poly(ADP-ribose) polymerase-1 inhibitor, 2-[3-[4-(4-chlorophenyl)-1-piperazinyl] propyl]-4(3H)-quinazolinone (FR255595), in an *in vitro* model of cell death and in mouse 1-methyl-4-phenyl-1,2,3,6-tetrahydropyridine model of Parkinson's disease. J Pharmacol Exp Ther;309:1067–1078.
13. Tamaoki S., Yamauchi Y., Nakano Y., Sakano S., Asagarasu A., Sato M. (2007) Pharmacological properties of 3-amino-5,6,7,8-tetrahydro-2-[4-[4-(quinolin-2-yl) piperazin-1-yl]butyl]quinazolin-4(3H)-one (TZB-30878), a novel therapeutic agent for diarrhea-predominant irritable bowel syndrome (IBS) and its effects on an experimental IBS model. J Pharmacol Exp Ther;322: 1315–1323.
14. Tobe M., Isobe Y., Tomizawa H., Nagasaki T., Takahashi H., Hayashi H. (2003) A novel structural class of potent inhibitors of NF-κB activation: structure–activity relationships and biological effects of 6-aminoquinazoline derivatives. Bioorg Med Chem;11:3869–3878.
15. Qian L., Shen Y., Chen J.-C., Wang Y.-X., Wu X.-T., Chen T.-J., Zheng K.-C. (2008) 3D-QSAR and docking studies of quinazoline derivatives with the inhibitory activity toward NF-κB. QSAR Comb Sci;27:984–995.
16. Rajput C.S., Singhal S. (2013) Synthesis, characterization, and anti-inflammatory activity of newer quinazolinone analogs. J Pharm;2013:1–7.
17. Madapa S., Tusi Z., Sridhar D., Kumar A., Siddiqi M.I., Srivastava K., Rizvi A., Tripathi R., Puri S.K., Shiva Keshava G.B., Shukla P.K., Batra S. (2009) Search for new pharmacophores for antimalarial activity. Part I: synthesis and antimalarial activity of new 2-methyl-6-ureido-4-quinolinamides. Bioorg Med Chem;17:203–221.
18. Domarkas J., Dudouit F., Williams C., Qiyu Q., Banerjee R., Brahimi F., Jean-Claude B.J. (2006) The combi-targeting concept: synthesis of stable nitrosoureas designed to inhibit the epidermal growth factor receptor (EGFR). J Med Chem;49:3544–3552.
19. Tsou H.R., Mamuya N., Johnson B.D., Reich M.F., Gruber B.C., Ye F., Nilakantan R., Shen R., Discafani C., DeBlanc R., Davis R., Koehn F.E., Greenberger L.M., Wang Y.F., Wissner A. (2001) 6-Substituted-4-(3-bromophenylamino)quinazolines as putative irreversible inhibitors of the epidermal growth factor receptor (EGFR) and human epidermal growth factor receptor (HER-2) tyrosine kinases with enhanced antitumor activity. J Med Chem;44:2719–2734.
20. Marvania B., Lee P.C., Chaniyara R., Dong H., Suman S., Kakadiya R., Chou T.C., Lee T.C., Shah A., Su T.L. (2011) Design, synthesis and antitumor evaluation of phenyl N-mustard-quinazoline conjugates. Bioorg Med Chem;19:1987–1998.
21. Smaill J.B., Palmer B.D., Rewcastle G.W., Denny W.A., McNamara D.J., Dobrusin E.M., Bridges A.J. *et al.* (1999) Tyrosine kinase inhibitors. 15. 4-(Phenylamino)quinazoline and 4-(phenylamino)pyrido[d]pyrimidine acrylamides as irreversible inhibitors of the ATP binding site of the epidermal growth factor receptor. J Med Chem;42:1803–1815.
22. Barnes M.C., Chana S.S., Dennison H., Mathews N., Spencer K.C. (2005) Morpholinylanilinoquinazoline derivatives for use as antiviral agents, 2005, US Patent number: US20080311076.
23. Botros S. (1972) Synthesis of certain nitro-quinazoline derivatives structurally related to some chemotherapeutic agents. Egypt J Pharm Sci;13:11–21.
24. Saad S.M., Khan I., Perveen S., Khan K.M., Yousuf S. (2013) N-(2,5-Dimeth-oxy-phen-yl)-6-nitro-quinazolin-4-amine. Acta Crystallogr Sect E Struct Rep Online;69: o8.
25. Foucourt A., Dubouilh-Benard C., Chosson E., Corbière C., Buquet C., Iannelli M., Leblond B., Marsais F., Besson T. (2010) Microwave-accelerated Dimroth rearrangement for the synthesis of 4-anilino-6-nitroquinazolines. Application to an efficient synthesis of a microtubule destabilizing agent. Tetrahedron;66:4495–4502.
26. Morley J., Simpson J. (1949) 215. The chemistry of simple heterocyclic systems. Part II. Condensations of 4-chloro-6-and 4-chloro-7-nitroquinazoline with amines. J Chem Soc;1014–1017.
27. Smaill J.B., Showalter H.D., Zhou H., Bridges A.J., McNamara D.J., Fry D.W., Nelson J.M., Sherwood V., Vincent P.W., Roberts B.J., Elliott W.L., Denny W.A. (2001) Tyrosine kinase inhibitors. 18. 6-Substituted 4-anilinoquinazolines and 4-anilinopyrido[3,4-d]pyrimidines as soluble, irreversible inhibitors of the epidermal growth factor receptor. J Med Chem;44:429–440.
28. Madapa S., Tusi Z., Mishra A., Srivastava K., Pandey S.K., Tripathi R., Puri S.K., Batra S. (2009a) Search for new pharmacophores for antimalarial activity. Part II: synthesis and antimalarial activity of new 6-ureido-4-anilinoquinazolines. Bioorg Med Chem;17:222–234.

29. Schnur R., Arnold L. (1996) Preparation of N-phenyl-quinazoline-4-amines as neoplasm inhibitors. US Patent number: WO9630347.
30. Boyce J., Brown M., Fitzner J., Kowski T. (2006) Kinase-directed, activity-based probes US Patent number: WO2006076463.
31. Pan Y., Wang Y., Cai L., Cai Y., Hu J., Yu C., Li J., Feng Z., Yang S., Li X., Liang G. (2012) Inhibition of high glucose-induced inflammatory response and macrophage infiltration by a novel curcumin derivative prevents renal injury in diabetic rats. Br J Pharmacol;166:1169–1182.
32. Wu J., Li J., Cai Y., Pan Y., Ye F., Zhang Y., Zhao Y., Yang S., Li X., Liang G. (2011) Evaluation and discovery of novel synthetic chalcone derivatives as anti-inflammatory agents. J Med Chem;54:8110–8123.
33. Gasparotto V., Castagliuolo I., Ferlin M.G. (2007). 3-substituted 7-phenyl-pyrroloquinolinones show potent cytotoxic activity in human cancer cell lines. J Med Chem;50:5509–5513.
34. Marshall H.E., Potts E.N., Kelleher Z.T., Stamler J.S., Foster W.M., Auten R.L. (2009) Protection from lipopolysaccharide-induced lung injury by augmentation of airway S-nitrosothiols. Am J Respir Crit Care Med;180:11–18.
35. Minamino T., Komuro I. (2006) Regeneration of the endothelium as a novel therapeutic strategy for acute lung injury. J Clin Invest;116:2316–2319.